Commissioning of the Photon Calibrators

Evan Goetz, T040196-00-D

Mentor: Daniel Sigg

Abstract

The photon calibrator system is designed to be an independent means to test the response of the LIGO interferometers to an external force. The applied external force is due to radiation pressure of photons recoiling off the end test masses. We want to know the interferometer response to this force as well as calibrate timing through the electronics. Calibration of the interferometer is crucial in order to deterimine gravitational wave parameters. The uncertainties of the overall calibration are determined by viewport window reflection, angle of incidence, test mass reflection, interferometer transfer functions, and amplitude of the calibration measurement. We compare the photon calibrator measurement to the current amplitude calibration measurement using the coil actuators.

1 Introduction

The LIGO interferometer is a long baseline power-recycled Michelson interferometer designed to detect gravitational waves from astrophysical sources. To achieve the sensitivity necessary to detect gravitational waves, LIGO implements Fabry-Perot cavities as the arms of the interferometers. Gravitational waves cause space-time to expand and contract which cause the mirrors to move from a stable position in space. In order to determine how gravitational waves effect the LIGO interferometer, we calibrate our signals with known measurements.

There are three methods to calibrate the interferometer to an absolute displacement. These are, fringe counting, fringe fitting and sign toggling. Fringe counting is useful for a calibration of 5-10 percent accuracy, while fringe fitting and sign toggling are more appropriate for a calibration accuracy of <5 percent. These methods use the coil actuators to drive the mirrors. [1]

To calibrate the interferometer using fringe counting, the interferometer is locked in a simple Michelson configuration with the free masses swinging. The calibration is obtained by observing the number of fringes that are crossed at the antisymmetric port and comparing this to the drive signal. Each bright fringe to bright fringe crossed corresponds to $\lambda/2$ drive assuming the drive dominates the mirror's motion. Fringe fitting uses the antisymmetric port signal data used from fringe counting and fits this to an algorithm to determine the calibration parameter. The sign toggling method uses a locked Michelson interferometer and a drive forces the antisymmetric port to go from bright to dark or vice-versa. This corresponds to a $\lambda/4$ drive. In this way a calibration can be obtained from the observed signal and drive.

There is a problem with these methods, however. The coil actuators are meant to stablize the mirror and hold it to a position in space. To calibrate the interferometer, we then drive the mirrors with the coil actuators. It becomes difficult to know how much force we exert on the mirror with a system such as the coil actuators.

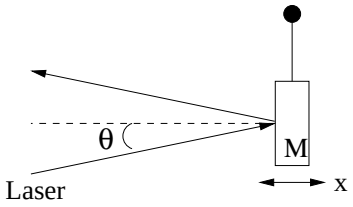

Figure 1: Setup of the photon calibrator with a laser hitting an ETM of mass M and causing a displacement of amplitude x.

An alternative to this technique is the photon calibrator system. This method uses radiation pressure due to recoiling photons to push on the end test masses (ETMs) with a known force. We modulate the power of the incident laser beam which results in a modulated force applied to the ETM. The mirror is assumed to be a simple pendulum and responds to this modulated force in a known way. In this manner the photon calibrator is an independent calibration technique.

The photon calibrator can be used as a complimentary system to the current methods of calibration. If the measurements plus error bars overlap, the we know the calibration is accurate. We can also test the timing of signals through the interferometer and electronics. Timing is crucial to determine location on the sky of the gravitational wave source and find useful, scientific data in the graviational wave channel.

This report details the calibration measurements and timing measurements made with the photon calibrator. We also report other useful techniques that may be possible with this device.

2 Theory of operation

The photon calibrator acts on the interferometer by dithering the ETMs with a power modulated laser beam. In this section, we detail the photon calibrator and the interferometer response.

2.1 Photon Calibrator

The ETM is pushed a small amount by the recoil of photons from the mirror surface (Figure 1). We know the force applied to the ETM due to radiation pressure is

$$F(t) = 2\cos\theta\frac{h\nu}{c}\dot{N}_\gamma \tag{1}$$

where θ is the angle of incidence of the laser beam, h is Plank's constant, ν is the frequency of the laser light, c is the speed of light and $\dot{N}_\gamma$ is the number of photons hitting the mirror per unit time. If we express this in terms of the power, P,

$$F(t) = 2\cos\theta\frac{P(t)}{c} \tag{2}$$

with the power of the laser beam written as,

$$P(t) = P_0 + P\cos\omega_c t \tag{3}$$

with ω_c as the angular frequency of the power modulated laser, P_0 is some DC power level and P is some power amplitude.

Let us assume that the ETM is a simple pendulum whose equation of motion can be written as

$$\ddot{x} + \gamma\dot{x} + \omega_0^2 x = y \tag{4}$$

where γ is a damping coefficient, $\omega_0^2 = g/l$ and y is given as

$$y = \frac{F(t)}{M} \tag{5}$$

where $F(t)$ is the force on the mass as a function of time and M is the mass of the ETM. Once we solve the equation of motion, we introduce the quality factor, $Q = \omega_0/\gamma$, and we write the displacement amplitude of the test mass as

$$x_c(\omega_c) = 2\cos\theta \frac{P}{cM} \frac{1}{\omega_p^2 - \omega_c^2 + i\omega_p\omega_c/Q} \approx -2\frac{\cos\theta P}{cM\omega_c^2} \text{ for } \omega_c \gg \omega_p \tag{6}$$

where ω_p is the angular pendular resonance frequency. [2]

If the calibration frequency is far from the resonant pendular frequency and the Q of the resonance is high, then we can take the approximation to be true. The measured pendular resonant frequencies and their undamped Q's are given in Table 1. This shows that the approximation we make is correct, since the photon calibrator has been designed to operate between 50 and 1000 Hz. Damping will not cause the frequencies to change, only the Q's, and since we are far from resonance, it will not effect our approximation.

Optic	**Pendular frequency**	**Q**
H1 ETMx	0.763 Hz	$\simeq$580
H1 ETMy	0.767 Hz	$\simeq$700
H2 ETMx	0.749 Hz	$\simeq$540
H2 ETMy	0.764 Hz	$\simeq$590

Table 1: Pendular resonant frequencies and Q's for ETM optics of LHO.

2.2 Interferometer Response

We assume that the interferometer responds to an external disturbance (such as a gravitational wave or the photon calibrator laser) with a simple feedback loop of gain $G(f)$. This can be idealized by three functions: the cavity response function, $C(f)$, which describes the response of the optical cavity, the digital filter function, $D(f)$, which describes the digital filtering and the actuation function, $A(f)$, which describes the mechanical response of the test masses. The relation of these three functions can be summarized as

$$G(f) = C(f) \cdot D(f) \cdot A(f) \tag{7}$$

Figure 2 shows a graphical interpretation.

Now, we assume that the time evolution of the calibration of the interferometer is a linear product of the optical gain in the instrument

$$C(f,t) = \alpha(t)C(f,t_0) \tag{8}$$

For the photon calibrator, a critical measurement is the uncertainty in α.

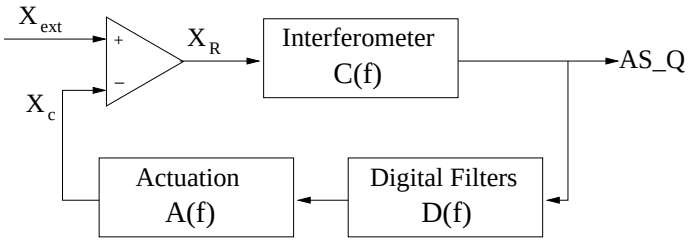

Figure 2: Block diagram of the LIGO interferometer servo loop.

To measure the uncertainty in α, we monitor the magnitude of our calibration line for a long period of time ($\sim$hours). We then measure the difference in values of the amplitude between consecutive minutes. These differences are histogrammed and the mean is taken to be the uncertainty in α. These errors are statistical so we can integrate for longer periods of time with a high signal to noise ratio to reduce this uncertainty. [3]

For the photon calibrator, the signal we see at the antisymmetric port (ASQ) is given by

$$ASQ = \frac{X_{ext}}{L_0}\frac{C(f)}{1+G(f)} \tag{9}$$

where $X_{ext} = L_x - L_y$ is an externally induced change in the differential arm length and L_0 is the arm cavity length. We can take $X_{ext} = x_c$ for the photon calibrator induced motion of the ETM.

2.3 Non-centered Photon Calibrator Beam

We have mounted the photon calibrator at viewports that allow the laser to be aimed at the ETMs on the 4km Hanford (H1) and 2km Hanford (H2) interferometers. For the H1 ETMs, we cannot align the laser beam at the center of the optic due to objects blocking the optical path. As such, our beam is about 4.1 cm off from center on H1 ETMx. This introduces a component of torque in the motion of the pendulum. On H2, there is nothing to block the optical path, so the mechancal torque is not an issue unless the beam is mis-aligned.

To analyze this, consider the torque on a mirror using the radiation pressure of a laser of power P, incident at an angle θ, that hits a mirror a distance d away from the center of the optic [4]

$$\tau = \frac{2Pd\cos\theta}{c} \tag{10}$$

The restoring torque of a torsion pendulum is written as

$$\begin{aligned} L &= I\dot{\beta} \\ \dot{L} = \tau &= I\ddot{\beta} \\ \tau &= \beta I\omega_y^2 \end{aligned} \tag{11}$$

where β is the angular displacement, I is the angular moment of inertia along the vertical axis and ω_y is the angular frequency in yaw. Solving for β and eliminating torque,

$$\beta = \frac{2Pd\cos\theta}{cI\omega_y^2} \tag{12}$$

The moment of inertia we are concerned with is along the x and y axis

$$I_{xx} = I_{yy} = \frac{1}{12}Mh^2 + \frac{1}{4}MR^2 \tag{13}$$

where for the ETMs, $M = 10.3$ kg, $h = 0.1$ meter and $R = 0.125$ meters. Table 2 gives the measured yaw resonant frequency for each ETM:

Optic	Yaw frequency
H1 ETMx	0.509 Hz
H1 ETMy	0.498 Hz
H2 ETMx	0.457 Hz
H2 ETMy	0.499 Hz

Table 2: Yaw resonant frequencies for ETM optics of LHO.

We assume that $P(t) = P_0 + P\cos\omega_c t$ so the angular displacement is dependent on P_0 for the DC angular displacement and P for the amplitude of the angular displacement. For the photon calibrator on the 4km ETMx, the amplitude of the angular displacement is on the order of 1e-16 radians.

3 Photon Calibrator Design and Methods

The photon calibrator laser is a horizontally polarized, 500mW, Nd:YLF which operates at 1047 nm. To modulate the power, the photon calibrator utilizes an acousto-optic modulator (AOM). The AOM allows the user to control the power, frequency and amplitude of modulated laser light that hits the ETM.

Within the photon calibrator enclosure, we have a power supply, AOM driver, a laser, a photodiode and optics which include two mirrors, two lenses, an AOM and a 99 percent reflective beam-splitter (Figure 3). We aim the beam using flat steering so the beam exits the enclosure and hits as near to the center of the ETM as possible. This minimizes effects of torsion on the optic and its suspension.

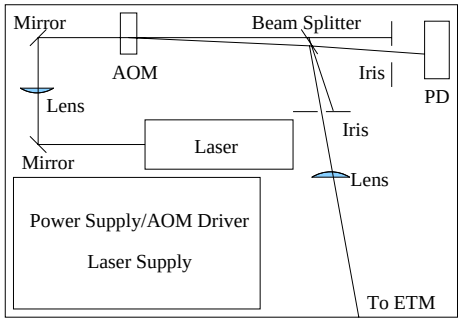

Figure 3: A schematic of the photon calibrator enclosure.

We make a calibration of the photon calibrator photodiode by measuring the output power with a power meter at various input power levels. This allows us to know how much laser power we aim at the ETM. A sample calibration is shown in Figure 5.

Figure 4: A photograph of the photon calibrator enclosure.

We have measured the transfer function of the photon calibrator read-back photodiode path using the arbitrary waveform generator. This plot is shown in Figure 6. Using the calibration and transfer functin, we know how the absolute power on the photon calibrator photodiode even as the modulation frequency varies.

Currently, we have mounted the photon calibrator on vertical posts which are attatched to the optical lever structure. We wanted to be sure the resonance features this may add to the optical lever signal would not appear in the ASQ signal. This has been shown to cause noise to appear in the optical lever signal and the ASQ signal at low frequencies. We discriminated between photon calibrator resonance peaks and other

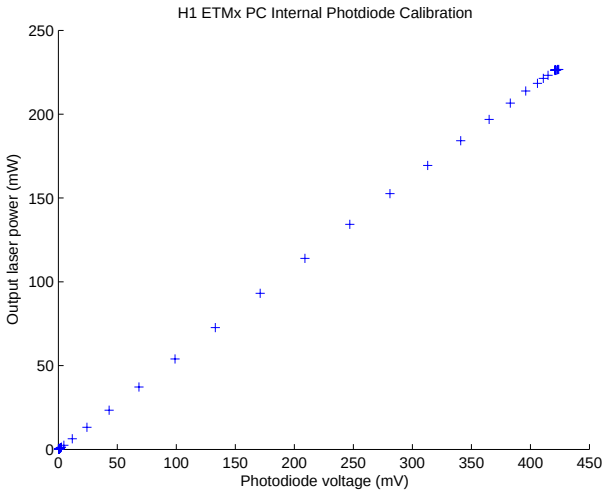

Figure 5: The H1 ETMx plot showing the calibration of the internal photodiode to output laser power.

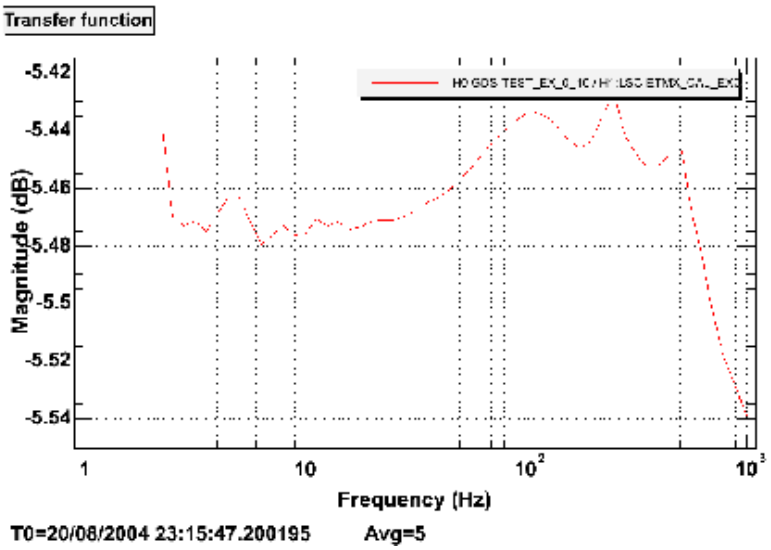

Figure 6: Transfer function of the AOM driver, AOM, photodiode and read-back channel.

resonant peaks by adding mass to the top of the photon calibrator which changes the resonant frequency peaks.

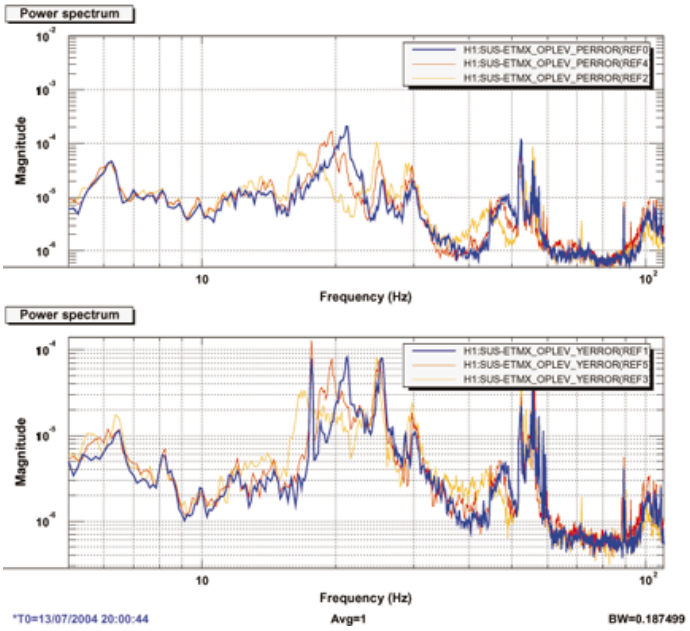

Figure 7: Optical lever signals with the blue trace having no extra mass while orange and red have more mass.

Figure 7 shows the optical lever signals with zero extra mass and two different masses ($\sim$2 kg and $\sim$5 kg) added to the top of the photon calibrator. The photon calibrator is responsible for the peak at about 21 Hz. We suspect this peak may be a torsional mode as the frequency dropped as we moved the mass from the center of the structure towards the edge. This resonance shows up in the ASQ signal (Figure 8). This suggests we need to construct new mountings for the photon calibrators which do not cause resonances to appear in the optical lever and ASQ signals or notch out the resonance. [5]

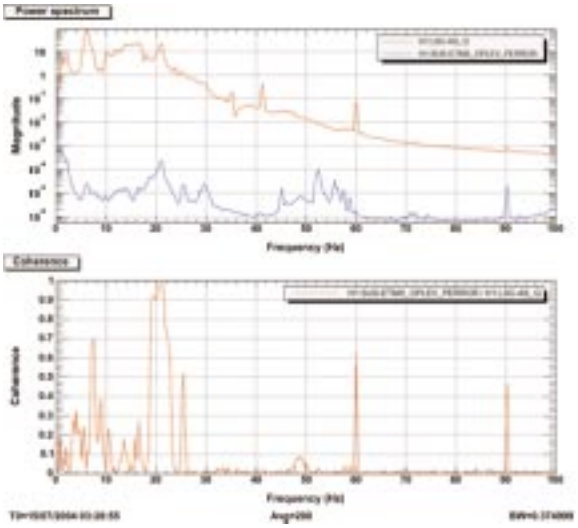

Figure 8: ASQ signals with coherence at 21 Hz likely due to the photon calibrator structure.

4 Data and Results

Our data is collected through two data channels of the LIGO data acquisition system (DAQ). The first data channel is the read-back photodiode that we read how much laser power we send out of the photon calibrator enclosure. The second data channel is the antisymmetric port photodiode (ASQ), which is the error signal data channel. Any calibration line, or swept sine measurement, should be seen in ASQ (when in common mode) provided it has significant amplitude and a frequency between 50 and 800 Hz. At higher frequencies, the amplitude of the modulated power must be increased since we are fighting the $1/f^2$ fall off of pendular response and $1/f$ fall off of the cavity response. All data has been collected from the H1 ETMx optic.

4.1 Calibration Line Measurement

First, we collect an "auto-calibration" (AutoCal) measurement of the interferometer to compare with the photon calibration measurement. Then we calculate an FFT of ASQ with the photon calibrator running (say at 141.0 Hz). We then measure the amplitude of the calibration line in the resultant FFT. This measurement is in counts(RMS)/ $\sqrt{\text{Hz}}$ and we convert this number to counts(peak).

Next, we find out how much amplitude power we reflect off the ETM by using the readback photodiode to tell us how much light is reflected out of the enclosure. The light that hits the viewport window has some

portion reflected. The reflected power has been measured on the 4k ETMx window to be 8.47 percent of incident power. We have measured the reflected power off the 4k ETMx to be 99.3 percent of incident by measuring the whitness plates in an optics lab setup. Taking these factors into account, we know how much the ETM is moved using the approximation in Eq. (6).

Finally, we divide the amplitude of motion (in meters) by the counts (peak) to find the calibration, X_{cal}, in meters/ct.

$$X_{cal} = \frac{x_c}{\sqrt{2(\mathrm{BW})}(\mathrm{ASQ})} \tag{14}$$

where BW is the bandwidth. For example, the calibration measured in Figure 9 was calculated from 0.108957 cts(RMS) /$\sqrt{\mathrm{Hz}}$. The motion we moved ETMx was calculated to be 1.3789e-16 meters. Thus the calibration is calculated to be 2.5311e-15 m/ct. We apply this calibration to the FFT and we compare the noise floor to the AutoCal noise floor. The ratio of the calibrated spectrum centered at 141.0 Hz is shown in Figure 10.

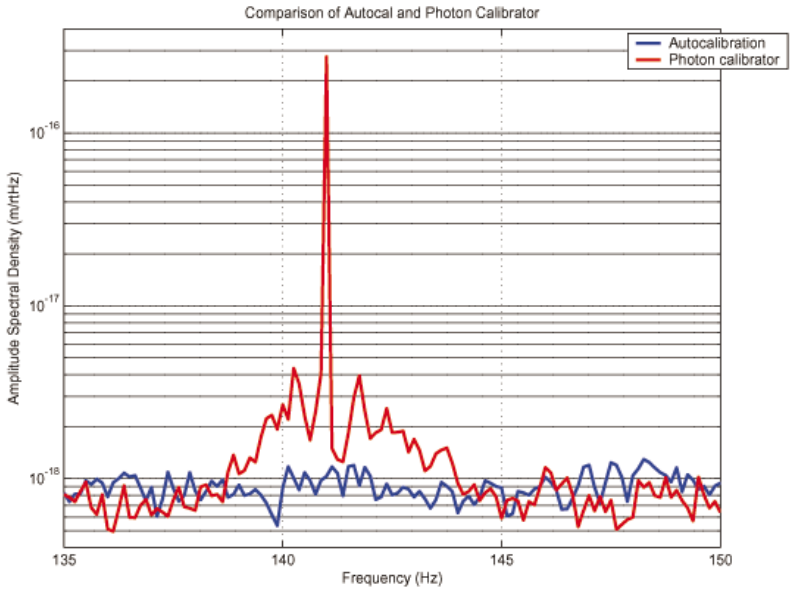

Figure 9: This plot compares the photon calibrator calibration measurement to the calibration made using AutoCal. There is good agreement on the amplitude of the noise floor.

We checked to make sure our calibration was valid at different drive amplitudes by calculating the ratio of the calibration. In the case where our calibrations were taken within a couple of minutes of one another, the variation was small ($\sim$2 percent). Calibrations taken with several days between had greater variation ($\sim$20 percent). This is due to a number of variables, but the optical gain and sensitivity of H1 had been increased between measurements and photon calibrator laser variability.

We have found that the power on the read-back photodiode of the photon calibrator has declined significantly ($\sim$60 percent). The photon calibrator laser had been running for 2 weeks continuously. This allowed us to monitor ther performance of the laser. We susupect the laser polarization to be changing or the laser itself is malfunctioning.

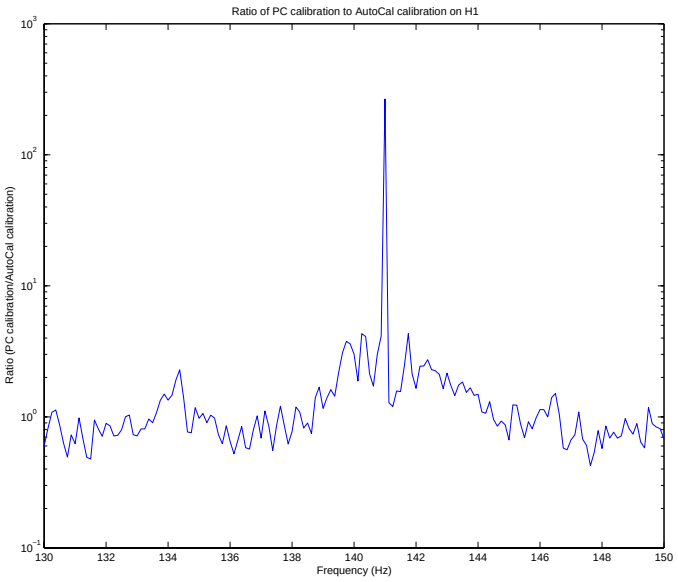

Figure 10: This plot compares the ratio of the photon calibrator calibration measurement to the calibration made using AutoCal. The peak is the photon calibrator line at 141.0 Hz which was not running when the AutoCal measurement was made so it appears in the ratio.

4.1.1 Calibration Uncertainties

There are several uncertainties which can be drived from Eq. (6) and others which are of an operational nature. For example, we know how much laser power we aim at the ETM from outside the vacuum assembly, but part of this light is reflected by the viewport and part of the light is not reflected by the ETM. These factors must be taken into account. Table 3 describes the uncertainties and estimated error.

4.2 Timing Measurements

The photon calibrator system can be used to measure time delays through the interferometer and electronics (Figure 11). This is done by measuring the phase difference between the read-back photodiode of the photon calibrator and the ASQ photodiode.

Time delay can be calculated from the phase difference by the equation

$$t = \frac{1}{f}\frac{\Delta\phi}{360^\circ} \tag{15}$$

where $\Delta\phi$ is the phase difference and f is the modulation frequency.

In our first tests, we measured the phase difference between the read-back photodiode of the photon calibrator and the ASQ signal. Figure 12 shows the results we measured in LIGO's data analysis software, DTT. For a modulation frequency of 141.0 Hz, we found the phase difference measured by DTT to be 16.7°. The pendular response lags by 180 degrees due to a high Q factor and low resonance frequency. Therefore,

Description	Variable	Estimated Error in Calibration
Laser Power reflected from ETM	P	6 percent
Test mass	M	negligible
Incident angle	θ	negligible
Speed of light	c	0
Frequency	ω_c	negligible
Viewport Reflection	P	5 percent
Amplitude of calibration line	α	10 percent (est.)

Table 3: Uncertainties in the calibration measurement.

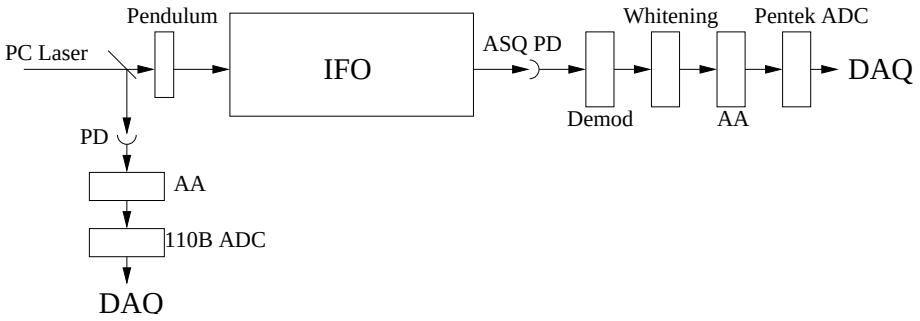

Figure 11: A schematic of the electronics and optics a signal must pass through before being read by the DAQ.

the phase difference is about 163.2 degrees. This corresponds to a time delay of 3.22 ms. See Table 4 for additional delay measurement data.

Next, we measured the transfer function of H1 between 50 Hz and 900 Hz. These plots (Figure 13) show the coherence and phase of our signals. We note that coherence drops below 0.9 at about 300 Hz. We likely need more integration time for the higher frequency signals in order to keep coherence above 0.9.

We have begun measuring the transfer functions in order to determine timing through the ASQ electronics chain. Figure 12 shows the transfer functions through some of the chain.

5 Future Improvement Suggestions

Further work on the photon calibrators will include the following:

- Measuring the error in amplitude of calibration line height. This has been explained in the interferometer response section of this document.
- We would like to measure the ratio of the calibrations at different calibration line amplitudes. This will help determine if there are any thermal effects due to heating of the ETM.
- Position on the ETM and size of the laser spot on the ETM may have different effects which we would like to investigate.

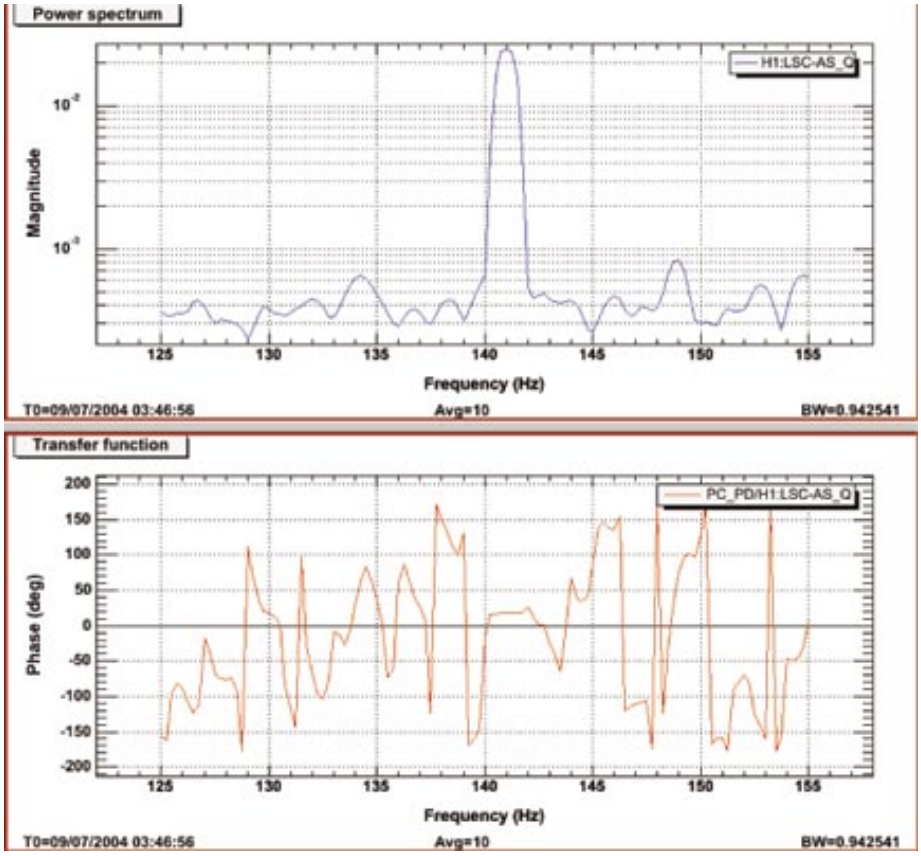

Figure 12: The phase delay for a 141.0 Hz calibration line injection. We show the magnitude of the signal seen in the uncalibrated ASQ spectrum and the phase delay at 141.0 Hz. The phase differnce seen at 141.0 Hz is about 16.7 degrees.

- As with the current LIGO setup, we would like to establish calibration lines at several different frequencies to monitor gain fluctuations.
- The AutoCal uses a swept sine measurement and fits the data to a model to find the calibration. This determines the closed loop transfer function. We can use the photon calibrator to do this same task. We would like to impliment a PhotoCal measurement to calibrate the interferometer in the same manner.
- Finish timing measurements of components in the photon calibrator and ASQ paths.
- Constructing a new framework to mount the PC would help reduce low frequency noise resonances in the optical lever channels and in ASQ.
- It is possible to inject artificial gravitational wave signals into the interferometer using the photon calibrator. One would have to know the waveform, polarization, phase, etc. of an artifical signal before injecting it into the interferometer. We can then observe the response of the interferometer to these artificial signals, and compare this to theoretical models of gravitational wave interactions.

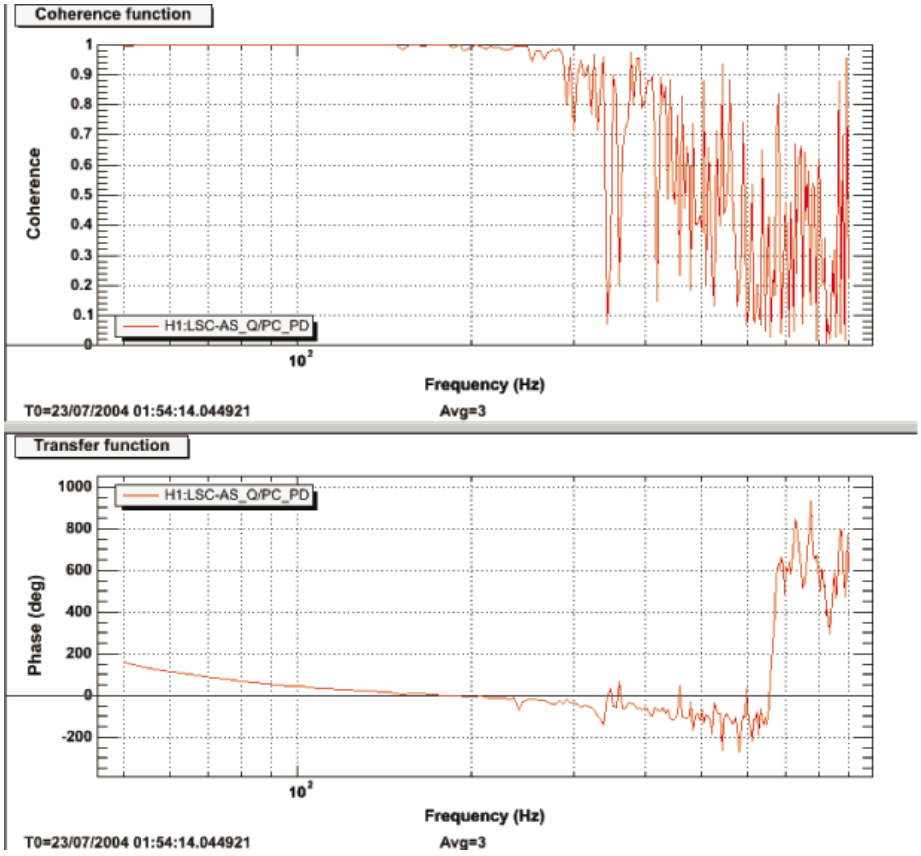

Figure 13: A plot of the coherence and phase of a swept sine measurement using the PC. Note that above 300 Hz the signals lose coherence. The data in the phase plot above 300 Hz is not accurate.

- A pseudo-random injection signal with an amplitude well below the interferometer noise levels avoids disadvantages of calibration lines by distributing energy over the entire gravitational wave band. Degradation of gravitational wave sensitivity would be negligible since disturbances are small and frequency independent. Both ETMs can be actuated independently and, in principle, give a calibration of both arms simultaneously. [2]
- Remote user control of the photon calibrator would be ideal, and this process should be implimented for the next science run.

6 Conclusions

We have shown the photon calibrator is a useful tool to perform calibration measurements on the LIGO interferometers. Our errors are managable and can be calculated from first principles. Timing measurements can also be done using the photon calibrator. The photon calibrator can be compared to the coil actuator calibration technique.

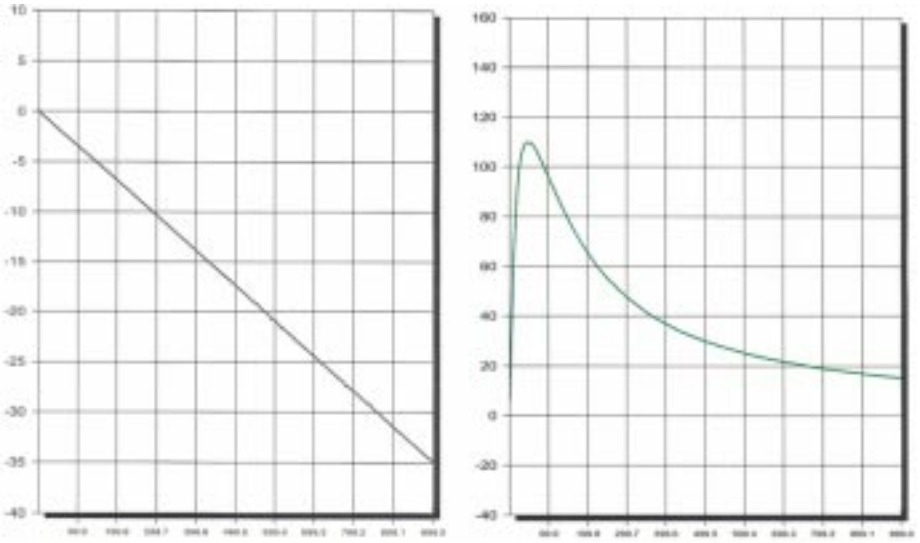

Figure 14: Phase delays through the antialiasing board (left) and the whitening board (right). The axes for these plots are frequency (Hz) on the x-axis and phase (degrees) on the y-axis.

Component	Delay
Pendulum	-180° ($>$50 Hz)
4km Interferometer	13.343 μs
Antialiasing board (ASQ)	86 μs
Whitening board (ASQ)	1.6 ms (at 141 Hz)
Antialiasing board (PC)	$<$5 μs
110B - Pentek ADC boards	$\simeq$ 70μs (relative difference)
Total delay measured	16.7° (at 141 Hz)

Table 4: Delays in the interferometer and electronics.

Acknowledgements I would like to thank Daniel Sigg, Michael Landry and Rick Savage for their advice on this project. This work is supported by the Research Experiences for Undergraduates (REU) of the National Science Foundation and the Summer Undergraduate Research Fellowships of the California Institute of Technology.

References

[1] Adhikari R, Evans M, Landry M, Marka S, Matone L and Yamamoto H, *Input Test Mass (ITM) Absolute Calibrations: Fringe Counting, Fringe Fitting, and Sign Toggling Methods* T020141-00-D

[2] Sigg D, *Strain Calibration in LIGO* T970101-B

[3] Gonzalez G, Landry M and O'Reilly B, *Calibration of the LIGO detectors for S2* T040060-00-D

[4] Sigg D, *Power-Induced Angular Shifts and Instabilities* T030039-00

[5] LHO Detector elog entry by Robert Schofield and Evan Goetz on 14 July 2004.